




Geomorphic signatures of active tectonics in Subansiri River Basin, eastern Himalayas

Diganta KUMAR  <https://orcid.org/0000-0002-4744-224X>; e-mail: digantakumar.digu@gmail.com

Bhagawat Pran DUARAH*  <https://orcid.org/0000-0002-3511-1451>;  e-mail: bpduarah@gmail.com

*Corresponding Author

Department of Geological Sciences, Gauhati University, Guwahati, Assam-781014, India

Citation: Kumar D, Duarah BP (2020) Geomorphic signatures of active tectonics in Subansiri River Basin eastern Himalayas. Journal of Mountain Science 17(6). <https://doi.org/10.1007/s11629-019-5492-x>

© Science Press, Institute of Mountain Hazards and Environment, CAS and Springer-Verlag GmbH Germany, part of Springer Nature 2020

Abstract: The Subansiri, a major tributary of the Brahmaputra with its catchment area (35763 km²) spreading almost entirely in the Eastern Himalayas across almost all the major and local tectonic features in the area witnesses large numbers of seismic events. Active tectonic indices like relief and slope, drainage pattern, longitudinal profile, valley profile, hypsometry, valley asymmetry factors and transverse topographic symmetry index, stream length gradient, valley floor-height ratio extracted from SRTM 3 arc-second data prove that the evolving basin morphology has substantial contribution from the Himalayan tectonics. Seismic data are incorporated in the study to establish the potentially active tectonic elements in the catchment area. The study shows that the western part of the Subansiri River Basin is profoundly tilted towards north in the upper catchment and towards east in the lower and middle part of the catchment. The predominant tectonic movements in the western part of the basin caused the tilting of the basin towards north in the upstream and towards east in the middle and lower parts.

Keywords: Eastern Himalayas; Active tectonics; Subansiri; Geomorphometry; SRTM DEM; Seismicity

Introduction

Geomorphic indices of a river basin are potentially good indicators of the evolving tectonic processes in the catchment area (Azor et al. 2002; Keller and Pinter 2002; Silva et al. 2003; Molin et al. 2004; Alipoor et al. 2011; Duarah and Phukan 2011; Mahmood and Gloaguen 2012; Kaushal et al. 2017; Srivastava et al. 2017; Kumar and Duarah 2019). Morphotectonic study of an active tectonic region includes application of mixed tools of geomorphology and river morphometry (Silva et al. 2003; Della Seta et al. 2008; Hamdouni et al. 2008). Drainage systems in most tectonically active areas are usually influenced by faults and their geometry as well as lithology (Schumm et al. 2000; Burbank and Anderson 2001; Maroukian et al. 2008), though hydrology has substantial contribution in giving shape to alluvial rivers. Mountain front sinuosity (*smf*) (Rockwell et al. 1985), valley floor width-height ratio (*Vf*) (Rockwell et al. 1985), valley asymmetry factor (*AF*) (Cox 1994), basin shape (*Bs*) and hypsometric integral (*HI*) (Strahler 1952), stream length gradient index (Hamdouni et al. 2008; Dehbozorgi et al. 2010; Hamdouni et al. 2010; Matoš et al. 2016) are important indices of relative active tectonics. In a tectonically active region the processes are continuous. Rigid deformation(s) in

Received: 27-Mar-2019
1stRevision: 02-Sep-2019
2nd Revision: 05-Dec-2019
Accepted: 05-Feb-2020

the crust results in the accumulation and release of stress as earthquakes. Hence earthquakes are the results of the past and current tectonic processes that shaped the current landscape and influenced the geometry of the river(s) present in that area.

The Subansiri (known as Tsari Chu in Tibet), a major Himalayan tributary of the Brahmaputra River, has a catchment area of about 35763 km² extending from Tibet (China) to India with 4237 km² (11.84%) of its area falling in the alluvial plains of the Brahmaputra valley in Assam (India). The river traverses across the South Tibetan Fault system (STF), South Tibetan Detachment system (STD), Main Central Thrust (MCT), Main Boundary Thrust (MBT), Main Frontal Thrust (MFT) and the catchment spreads over Higher, Lesser and Sub-Himalayas (Figure 1). After traversing through the Miri Hills in the outer Himalaya (Siwalik foothills) the river debouches into the alluvial plains of Brahmaputra at Dulangmukh in Assam at an elevation of 94 m above msl. The river is 208 km long in the Himalayan part and it originates at an altitude of 4200 m asl.

The present work is carried out to evaluate the contribution of tectonic features and processes in the catchment of the river on the basis of geomorphology and geomorphometric parameters. During the study, supports of earthquake data are also taken to evaluate the tectonic features.

1 Study Area, Geology and Tectonic Setting

The study area is bounded between latitudes 26° 45' N and 29° N and longitudes 91° 30' E and 95° 30' E in the eastern Himalayas (Figure 1). The lithotectonic settings discussed in the 'Seismotectonics Atlas of India and its Environs' (GSI 2000) are adopted to establish the interrelations of geomorphological and geomorphometric results with lithotectonic settings. The lithotectonic units are separated by major tectonic features and results in unique representative unit of the terrain. This gives advantages of interpretation over the rock units which are mingled through complex history of geological evolution of the terrain much before the continent-continent collision and also after the

collision. The northernmost part of the basin is located on east-west trending "older cover sequence affected by Himalayan fold-thrust movement" (GSI 2000). Immediate south of this sequence is the nearly east-west trending "crystalline complex overprinted by Himalayan fold-thrust movement" that occupies the upper Subansiri basin. Towards south the sequence is bounded by the Main Central Thrust (MCT), the other side of which is occupied by "older folded cover Palaeozoic-Mesozoic sequence overprinted by Himalayan fold-thrust movement, the southern limit of which is marked by MBT-2 (Figure 1). This part of the basin is named 'middle Subansiri basin' in the article where the Subansiri traverses across nearly NE-SW trending tectonic features. Further south is a narrow belt of "older folded cover Mesozoic sequence overprinted by Himalayan fold-thrust movement" between MBT2 and MBT3 followed by Gondwana and Siwalik sequences demarcated together as "cover rocks of frontal belt of Himalaya affected by fold-thrust movement during terminal phase of Himalayan orogeny". Alluvial fill along the foredeep is only seen in the plains of Brahmaputra.

The tectonic settings of northeast part of India are unique due to presence of two collision zones with distinct and different tectonic settings (Kayal 1998; Angelier and Baruah 2009). The area has witnessed many devastating earthquakes including two great earthquakes with magnitudes around 8.5 in 1897 in Shillong Plateau (Oldham 1899; Bilham and England 2001; Rajendran et al. 2004) and in 1950 near Rima, Arunachal Pradesh (Poddar 1950; Tandon 1955; Ben-Menahem et al. 1974) though their epicentres were at distant places outside the Subansiri catchment. The catchment witnessed a major earthquake of magnitude 7.3 (ISC 2017) on 29 July in 1947 near Taksing in Arunachal Pradesh.

The major tectonic elements in this part of the Himalayas from south to north (Figure 1) includes: 1) Main Frontal Thrust (MFT) which separates the Brahmaputra Alluvium and Siwalik rocks; 2) Main Boundary Thrust (MBT) along which the older rocks from the north thrust over the folded Cenozoic Siwalik rocks (Das 2004); 3) Lesser Himalayan Thrust Zone (LHZ) (Yin 2006); 4) Main Central Thrust (MCT) separating the older folded cover sequences of Lesser Himalayas and Crystalline Complex of Greater Himalayan

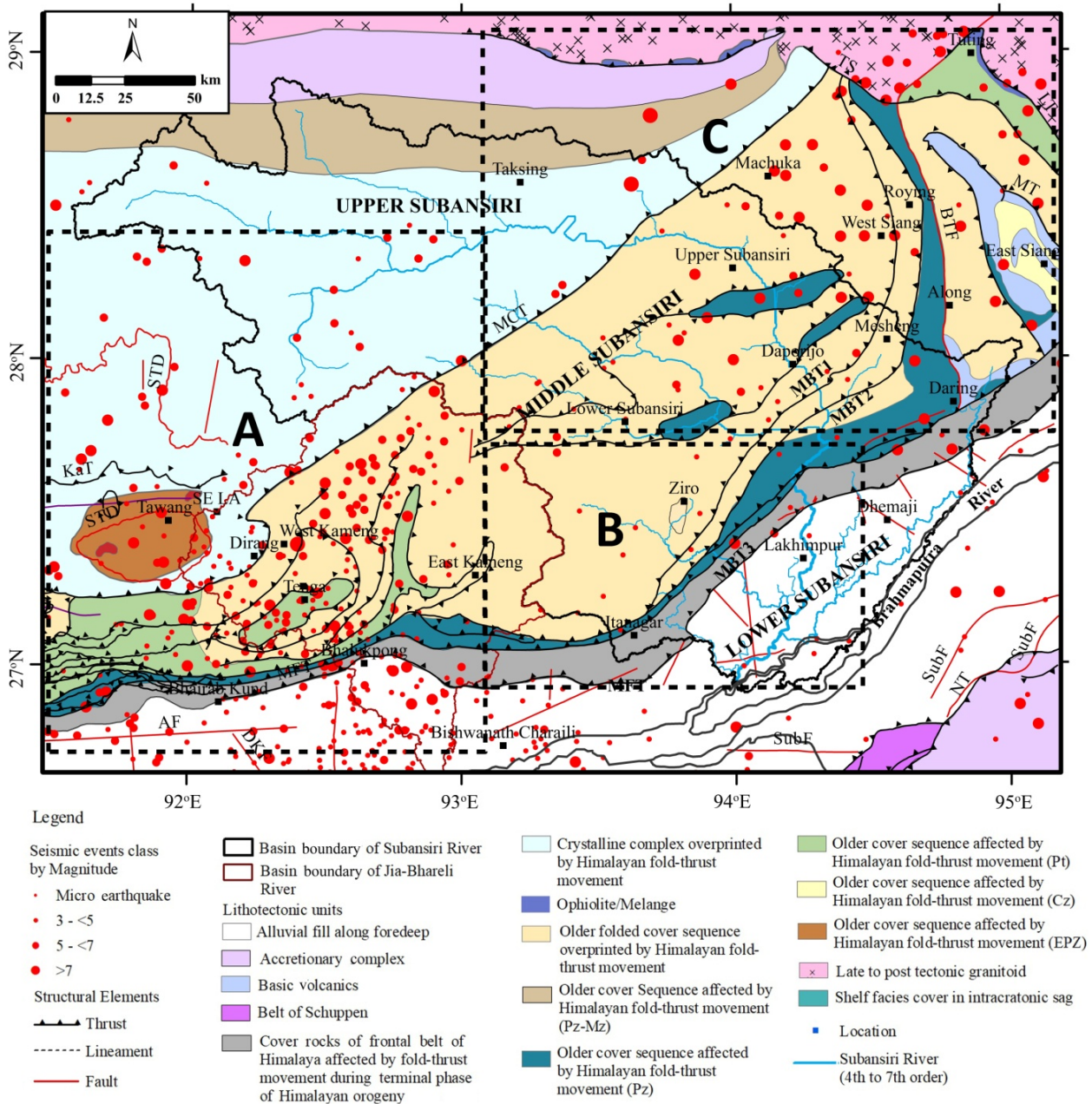


Figure 1 Litho-tectonic map of the Subansiri River Basin. The earthquake epicenters are plotted and symbolized according to their magnitude. Data base: GSI (2000); USGS (<http://earthquake.usgs.gov/search/>); ISC (<http://www.isc.ac.uk/iscbulletin/search/catalogue/>); NEIST (2012) and Long et al. (2011). The thick dashed-line rectangles represented by the letters A, B and C are three tectonic domains discussed here. **Abbreviations:** MCT- Main Central Thrust; MFT- Main Frontal Thrust; MT- Mishmi Thrust; MBT- Main Boundary Thrust; MBT1-MBT2-MBT3 – are the bifurcated branches of Main Boundary Thrust; NT- Naga Thrust; KaT - Kakhtang Thrust; SubF – Subsurface Fault; STD - South Tibetan detachment; MM- Mishimi Massif; TP – Tibetan Plateau; Pt – Proterozoic; EPZ – Early Paleozoic; Pz – Paleozoic; Mz – Mesozoic; Cz – Cenozoic.

sequences (GSI 2000); 5) the South Tibetan Fault system (STF); and 6) South Tibetan Detachment system (STD). The major structures in this part of Eastern Himalayas dominantly have east-west trend in the western part, which swings in the

eastern part to the northeast and then almost to the north before abutting against the Mishimi Thrust and Tidding Suture (the western boundaries of the trans-Himalayan Mishimi Massif). The epicentral plots on the litho-tectonic map (Figure 1) shows

that the Subansiri River Basin represents a seismically active area where recent micro-seismic events spread over the entire river basin, barring certain parts towards the north.

2 Data Sources and Morphometric Parameter Selection

2.1 Data sources

The 3 arc-second SRTM DEM, Landsat 7 ETM+, Landsat 8 OLI and TIRS digital data, published maps and Survey of India toposheets are used in the present study. The morphometric parameters of the Subansiri and its tributaries are extracted from 3 arc-second SRTM (void filled by "SRTM FILL" software, <http://3dnature.com/index.php/downloads/srtmfill-tool/>) data. SRTM DEM data are useful in hydrology and geomorphological analysis (Hancock et al. 2006; Liu 2008). Also, the accuracy of the both 30 m and 90 m resolution SRTM data are found identical in mountainous region (Mukul et al. 2016). The morphometric parameters are extracted using RiverTools 3.0 software (RIVIX 2005) which is a user-friendly GIS software for analysis and visualization of digital elevation model, watersheds and river networks. One of RiverTools' most powerful features is its ability to rapidly extract drainage network patterns and analyze hydrologic data from very large digital elevation models (DEMs). RiverTools provides accurate measurement of river and basin characteristics such as upstream area, channel lengths, elevation drops, slope and curvature using the Earth ellipsoid model of one's choice.

The lithotectonic map has been prepared from the published "Seismotectonic Atlas of India and its surrounding region" (GSI 2000). The geological structures are plotted from GSI (2000), Misra (2012) and also from satellite image interpretation. The earthquake epicenter data from 1908-2016 are adopted from United States Geological Survey, USGS (<http://earthquake.usgs.gov/earthquakes/search/>) and ISC (International seismological Center, ISC (<http://www.isc.ac.uk/iscbulletin/search/catalogue/>)). Apart from these seismic events, few historical events have also been

included in this study.

In this study the Subansiri River Basin is divided into three tectonically and lithologically homogeneous domains for the purpose of convenience in interpretation: 1) upper Subansiri River Basin, which covers Higher Himalaya the north of the MCT; 2) middle Subansiri River Basin, which covers the Lesser Himalayan part in between MCT and MBT and 3) the lower Subansiri River Basin, which includes the foothills region along with the alluvial plains. The study is restricted for 5th or higher order sub-basins.

2.2 Morphometric parameters

The geometric characteristics of a master channel and its tributaries are called basin morphometry. The quantifiable set of geometric properties of each basin defines the linear, areal and relief characteristics of the catchment and these are known as the basin morphometry. Keller and Pinter (2002) defined morphometry as the quantitative measurement of landscape shape which allows the objective comparison of the landform. Different morphotectonic parameters included in this study are – (a) stream order, (b) drainage pattern, (c) longitudinal profile, (d) valley profile, (e) hypsometry, (f) valley asymmetry factors and transverse topographic symmetry, (g) stream length gradient, (h) ratio of valley floor and valley height, and (i) relief and slope.

2.2.1 Delineation of drainage basin

The drainage system records all the information about landscape changes and the evolution of faults and folds (Ollier 1981; Leeder and Jackson 1993). Drainage or channel pattern can be defined as the particular plane or design that the individual stream courses can collectively form as it adopts the landform changes. In RiverTools 3.0, river network is extracted from DEM by extracting flow grid which shows flow direction of water pixel wise, defining basin boundary by marking basin divides from flow grids and finally applying the pruning method and defining threshold to determine attributes for every link and Strahler stream order in the selected basin. Common kinds of drainage patterns are the dendritic, trellis, rectangular and radial along with few other patterns which are combination of two or

more (Howard 1967; Bloom 2003; Tidwale 2004).

2.2.2 Relief and slope

DEM contains the elevation information above mean sea level against particular geographic location. Elevation is considered as basic topographic parameter (Ruszkiczay-Rüdiger et al. 2009) which defines the surface runoff. Elevation is considered as the starting point of the DEM based morphometric analysis (Ruszkiczay-Rüdiger et al. 2009). Relief is defined as the difference in elevation within a certain areas ($h_{max}-h_{min}$). Relative relief map of the Subansiri River basin and its surrounding area was analysed with Zonal Statistics using 1000m² grid.

Slope is the gradient of a particular area independently from the elevation above sea level (Adediran et al. 2004; Ruszkiczay-Rüdiger et al. 2009) and is the first derivative of the elevation. Slope variability is defined as the difference between maximum and minimum slopes within a particular area ($slope_{max} - slope_{min}$) which is computed using zonal statistics for 1000 m² grid.

2.2.3 Valley asymmetry factor (AF)

Valley asymmetry factor (AF) is a quantitative index to evaluate tectonic tilt in a basin (Keller and Pinter 2002). It is defined as

$$AF = 100 (A_r/A_t) \quad (1)$$

where A_r is the area of the basin to the right (facing downstream) of the trunk channel, and A_t is the total area of the drainage basin. The value of asymmetry factor nearer to 50 is considered as the 'symmetric basin' (Keller and Pinter 2002). Pérez-Peña et al. (2010) modified the valley asymmetry factor (AF) equation to

$$AF = |50 - A_r \times 100 / A_t| \quad (2)$$

Pérez-Peña et al. (2010) proposed classification scheme for valley asymmetry: symmetric ($AF < 5$), gently asymmetric ($5 \leq AF < 10$), moderately asymmetric ($10 \leq AF < 15$) and strongly asymmetric basin ($AF \geq 15$).

2.2.4 Transverse topographic symmetry (T)

Cox (1994) adopted transverse topographic symmetry to study the tilting of river in the valley part. It is defined as

$$T = D_a/D_d \quad (3)$$

where D_a is the distance from the midline of the

drainage basin to the midline of the active meander belt and D_d is the distance from the basin midline to the basin divide. For perfectly symmetric basin $T=0$ and it approaches 1 as asymmetry increases. Several transverse topographic symmetry sections were considered which were selected according to the shift of the channels.

2.2.5 Longitudinal profiles

Longitudinal profile of a river is explained as gradient of the water surface line from source to mouth. Here elevation data are plotted against the distance along the stream channel. Streams with increasing discharge in the downstream shows concave longitudinal profile. Sudden drop of the elevation in the longitudinal profile infers changes in lithology or presence of geological structures like fault or other influential factors like climatic change. The near vertical section along the longitudinal profile is known as 'knickpoint' which are made visible by the presence of waterfalls. In this study, longitudinal profiles were drawn using 3 arc-second SRTM DEM and RiverTools 3.0 software. Since in a normal section the longitudinal profile smoothens and kinckpoints are difficult to identify, the vertical scale of the longitudinal profiles are exaggerated. The constructed longitudinal profiles were normalized by following Demoulin (1998), Ruszkiczay-Rüdiger et al. (2009) and Matoš et al. (2016). Here distance along the valley (l) is normalized to the total channel length (L), l/L and elevation (e) is normalized to total height of the basin (E), e/E . Longitudinal profile concavity factors (C_f), maximal concavity (C_{max}) and the distance of the C_{max} from the source of the river along the abscissa (l/L) were calculated (Matoš et al. 2016) from the normalized longitudinal profile. The C_{max} value is derived as the maximum vertical difference between the normalised longitudinal profile and the diagonal line joining the source to the end point of the river profile. The ratio of the area bounded by the normalized longitudinal profile, the diagonal line and the C_{max} line to the total area bounded between the normalized longitudinal profile and the diagonal line in terms of percentage is defined as Concavity factor (C_f). C_f value generally ranges from 0% to 100% while maximal concavity (C_{max}) ranges from 0 to 1. High C_f and C_{max} values indicate that the river attains a graded profile, while lower

values suggest that the profile is possibly influenced by either active tectonic or lithological control (Demoulin 1998; Rãdoane et al. 2003; Ruzkiczay-Rüdiger et al. 2009). Graded rivers have small l/L values. A bi-variant scattered plot of C_{max} and l/L is also plotted to compare river characteristics.

2.2.6 Valley profile

A straight reach of a river without any confluence of its tributaries usually is deflected by changes in slope or elevation along its course. The river valley profile is a plot of elevation against the distance across a river. So, cross sectional profiles taken from right bank to left bank where there is no confluence of tributaries shed lights into the history of tilting of the basin, thus yield valuable information on the tectonic history of the basin. Valley profile shows stepper slopes in the elevated parts whereas gentle slope on the leveled terrain. The valley profiles were derived using 3 arc-second SRTM DEM and GIS software and examined to infer the probable tilt. An asymmetrical valley profile may be developed due to shifting of the channel thalweg towards a side of the river caused by – (a) erosion of concave side of a meander, or by (b) tectonic down tilting of the river basin towards that side (Duarah and Phukan 2011; Kumar and Duarah 2019). The valley profiles are drawn in straight sections of the present rivers to avoid the effects of meandering erosion. In a tilted valley the river cuts the toe of the bank towards which down tilt occurs that result a steep bank in the direction of tilt and gentle slope in the opposite bank.

2.2.7. Hypsometry

Hypsometry tells about the distribution of surface area or horizontal cross sectional area of a landmass with respect to the elevation. The modal hypsometric equation using percentage hypsometric curves (Strahler 1952) is given in the form

$$y = \left(\frac{d-x}{x} \times \frac{a}{d-a} \right)^z \quad r = \frac{a}{d} = 0.1 \quad (4)$$

where a and d are constants, d always greater than a , and the exponent z , positive or zero. The slope of the curve at its inflection point depends on the ratio $\frac{a}{d}$ (designated by r). In simple terms the hypsometric curve is plotted by taking - (1) the ratio of area between a contour and the upper perimeter (area ' a ') to total drainage basin area

(area ' A ') which is defined as 'relative area' and represented by the abscissa on the coordinate system; and (2) the ratio of height of contour above base (h) to total height of basin (H) which is defined as 'relative height', represented by values of the ordinate (Strahler 1952).

A convex curve signifies that most of the area within the basin has relatively higher elevation (upliftment exceeds erosion); alternatively, a concave curve indicates relatively lower elevated area (erosion exceeds upliftment). Integration of the percentage hypsometric curve (Eq.(4)) gives hypsometric integral (HI) (Strahler 1952) in the following form (Brocklehurst and Whipple 2004)

$$HI = \frac{\bar{Z} - Z_o}{Z_{max} - Z_o} \quad (5)$$

where HI is the hypsometric integral, Z_{max} is the maximum elevation of the catchment, \bar{Z} is the average elevation and Z_o is the minimum or outlet elevation. HI values range from 0 to 1. HI value '0' means extremely old topography while value '1' infers youngest topography. High HI value and convex up hypsometric curve indicate younger topography (Strahler 1952).

2.2.8 Valley floor width-height ratio (V_f)

The ratio of the valley width and the valley height of a river basin (Bull and McFadden 1977; Bull 1978) " V_f " is mathematically expressed as

$$V_f = 2V_{fw} / [(E_{ld} - E_{sc}) + (E_{rd} - E_{sc})] \quad (6)$$

where E_{ld} and E_{rd} are the elevations of the left and right side of the basin respectively; E_{sc} is the average elevation of the valley floor; and V_{fw} is width of the valley floor. A steep V-shaped valley has high V_f index while it is low in a wide U-shaped valley. With higher rate of upliftment and deep incision the V_f value decreases. The V_f values are calculated for the 4th order sub-basins only in the mountainous sections, and the alluvial part is avoided since this is strongly influenced by fluvial process.

2.2.9 Stream length gradient (SL) index

The SL index (Hack 1973) is one of the quantitative geomorphic parameters which can be defined as

$$SL = (\Delta H / \Delta L) \times L \quad (7)$$

where $(\Delta H / \Delta L)$ is the local slope of a channel segment and L is the length of the channel from the water divide to the midpoint of the channel reach

and is a quantitative measure for geomorphic processes related to erosion and deposition. In this study ΔH , ΔL and L measurements are made in meters. Higher SL values are resulted from active upliftment and/or the presence of higher resistance rocks in the area (Keller and Pinter 2002) and lower SL values indicates lower rock resistance or river flowing parallel to the structure *viz.*, landform made by strike-slip valley (Alipoor et al. 2011). Hence SL can be used as a tool to detect local uplift as well as the incipient local response to regional processes (Troiani and Della Seta 2008). Stream length gradient ($\Delta H/\Delta L$) is also used as it gives the steepness of the channel in segments.

3 Results

The 7th order Subansiri River has 30 numbers of 4th order sub-basins, 7 numbers of 5th order sub-basins and 3 numbers of 6th order sub-basins.

3.1 Relief and slope

Relief of the Subansiri River (Figure 2a) demonstrates that the northern upper part of the basin has elevations exceeding 6000 meter which drops down as low as 76 meter above msl in its confluence with the Brahmaputra. The high relief areas are occupied by Crystalline Complex of the Higher Himalayas and the moderate relief areas are mostly occupied by older cover sequences of the Lesser Himalayas in the south of the Higher

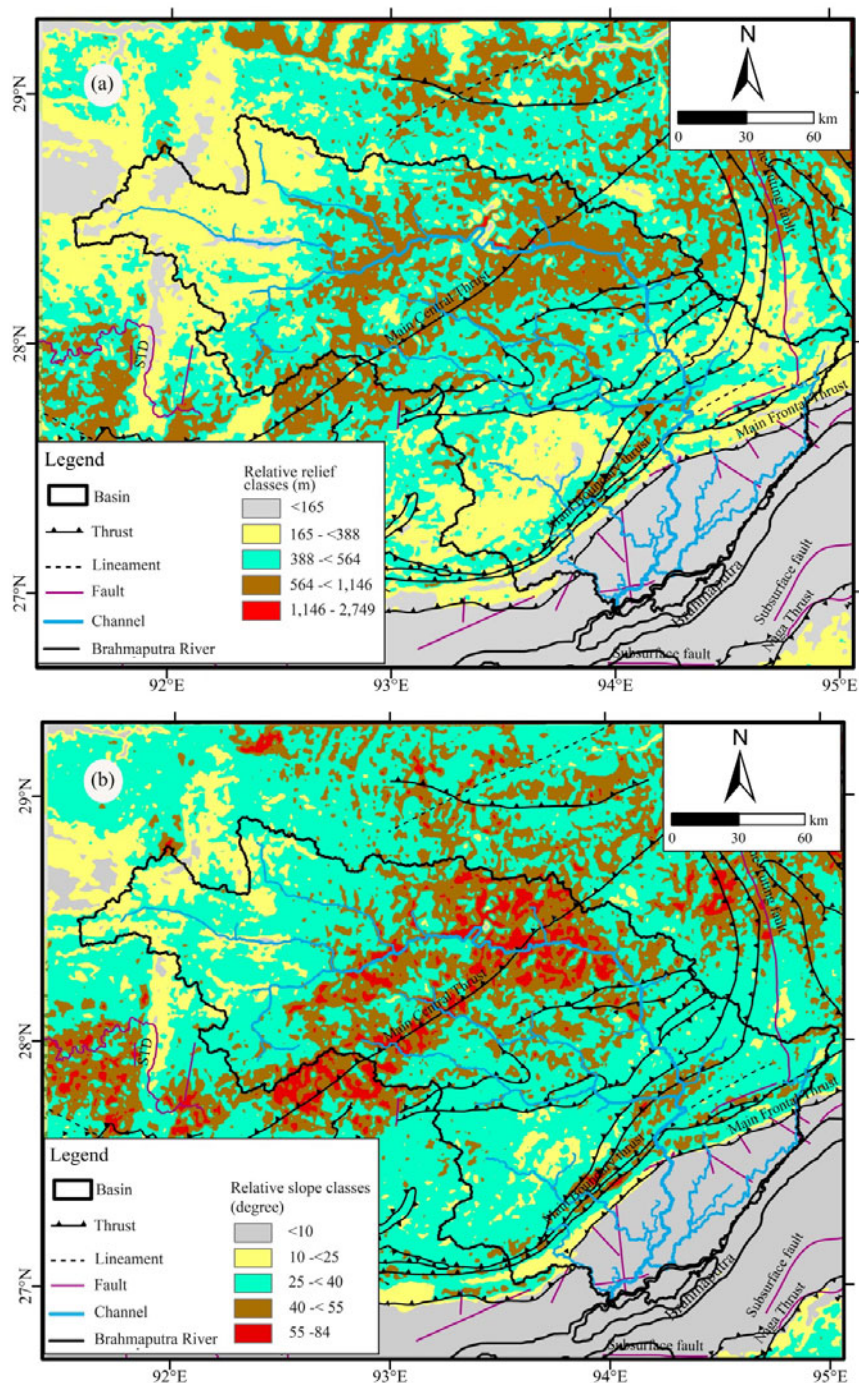


Figure 2 a) Map of relative relief (in meter of the Subansiri River based on zonal statistics in 1000 m² grid. b) Relative slope map of the Subansiri River based on zonal statistics in 1000 m² grid. Tectonic elements are superimposed to show the relationships of slope and relief to the major structural elements.

Himalayas and further south the Himalayan foothills contain sedimentary sequences with relief variations of 500-1500 meter. The relative relief is the local relief of an area and in the present study is worked out taking grids of 1000m². The relative relief map (Figure 2a) shows that average local relief

is higher on the middle part of the Subansiri basin. The relative relief on the middle Subansiri basin is ranging from moderate to high (388 - < 564m, 564 - <1146m and 1146 - 2749m; Figure 2a). The upper part of the Subansiri basin possesses low local relief (<388m Figure 2a). However, the relative relief of the upper Subansiri basin along the Main Central Thrust is moderate to high (564 - <1146m and 1146 - 2749 m). The upper part of the lower Subansiri basin (foothills of Arunachal Pradesh) possesses mostly lower local relief (<388 m; Figure 2a).

The slope-angle variability map (Figure 2b) shows that higher terrain roughness in the middle part of the Subansiri basin and also in the lower part (towards MCT) of the upper Subansiri basin (slope-angle classes are 25° - <40°, 40° - <55° and 55° - <84° ; Figure 2b). The area along the Main Central Thrust (MCT) shows higher slope-angle classes of slope ranges 40° - <55° and 55° - <84° (Figure 2b).

3.2 Drainage pattern

The geological structures present in the area guide the flow pattern of the drainage system (Figure 3) and therefore can be used to retrieve information about the evolution of structures proceeding from the analysis of drainage system to geological structures (Ollier 1981; Ledder and Jackson 1993). The river channels follow major and regional structural trends of the Himalayas and channel patterns change with the changed situation of lithology and tectonic elements.

In the Subansiri River system the channel patterns are mainly rectangular types (Figure 3a), trellis (Figure 3b) and dendritic (Figure 3c). The rectangular pattern dominates over the dendritic pattern in western and northern parts of the basin. The rectangular drainage pattern is generally seen in the areas with rectangular arrangement of faults and joints (Thornbury 1989). Dendritic pattern

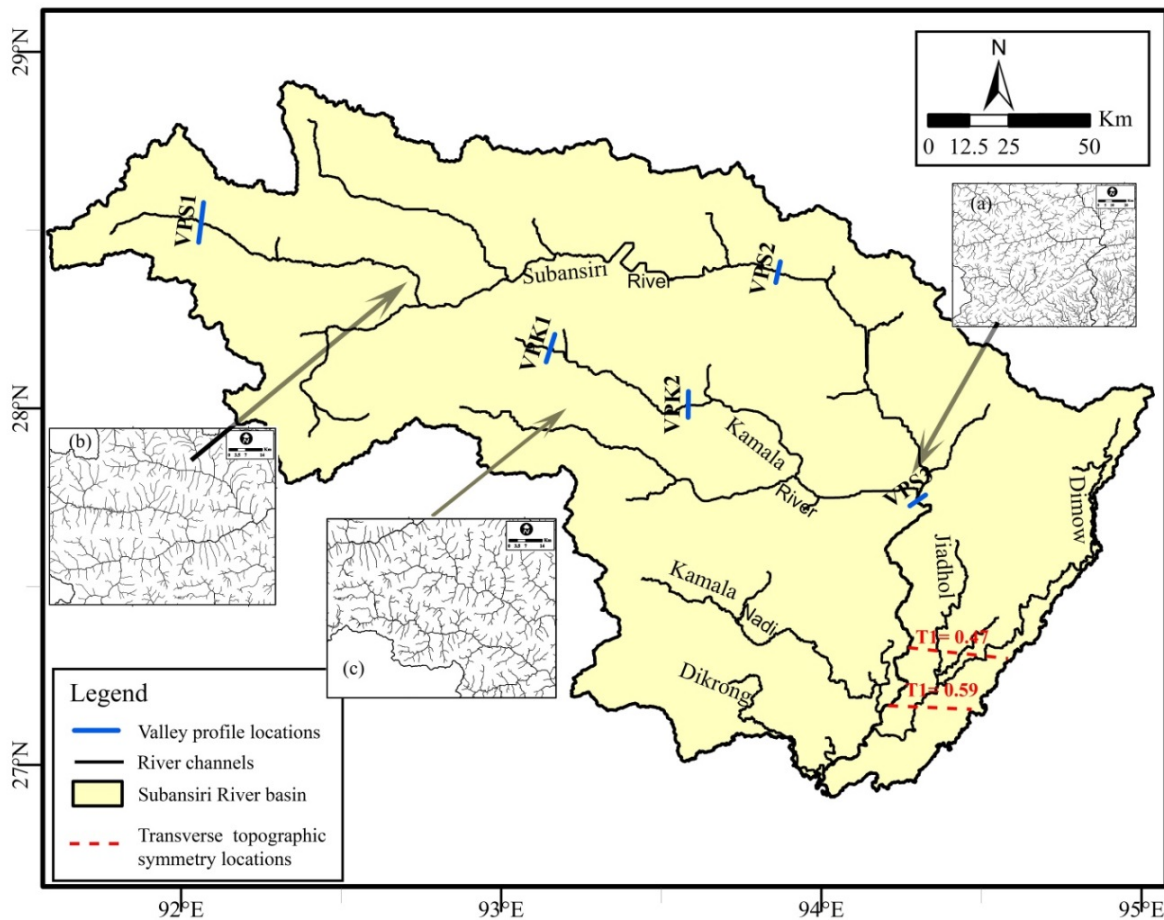


Figure 3 Drainage map of the Subansiri River. VPS1, VPS2, VPS3 – valley profiles of Subansiri; VPK1, VPK2 – valley profiles of Kamala, a tributary of the Subansiri. Common drainage patterns found in the Subansiri are – (a) rectangular, (b) trellis and (c) dendritic.

with subdued rectangular component are mainly seen in the middle part of the lower reach of the Subansiri basin whereas the central part of the upper reach of the river mainly possesses trellis drainage pattern. In the foothill region the predominant drainage pattern is parallel type and in the Brahmaputra plains the channels show dendritic pattern. The trellis pattern is mainly developed on the Crystalline Complex. The dendritic pattern is also found developed in the areas of eroded Crystalline Complex with gentle slope and older folded cover sequences of the Himalayas in the Lesser Himalayas.

3.3 Longitudinal profiles

Seven longitudinal profiles have been drawn from seven different river channels – the Subansiri and five of its tributaries, namely, the Kamla, the

Ranganadi, the Dikrong, the Jiadhah, the Dimow and a tributary of the Kamla River. The Dikrong and Ranganadi rivers debouch to the Subansiri in the Brahmaputra alluvial plain (Figure 4). The Jiadhah and the Dimow rivers together form the Charikaria River which finally debouches to the Subansiri River in the Brahmaputra plains. The concavity factor (C_f) of the seven normalized longitudinal profiles varies from 31.50% to 81.42% with mean 66.67%. The normalized longitudinal profile of the Subansiri River has lowest C_f value while the other tributaries have higher C_f values with the Jaidhal possessing the highest. The lowest C_{max} value is 0.37 and found in the middle reach of the Subansiri basin. The C_{max} values of the tributaries of the Subansiri range from 0.42 to 0.69.

The number of knickpoints of the seven longitudinal profiles (Figure 5) with its geographic location and its association with the faults present

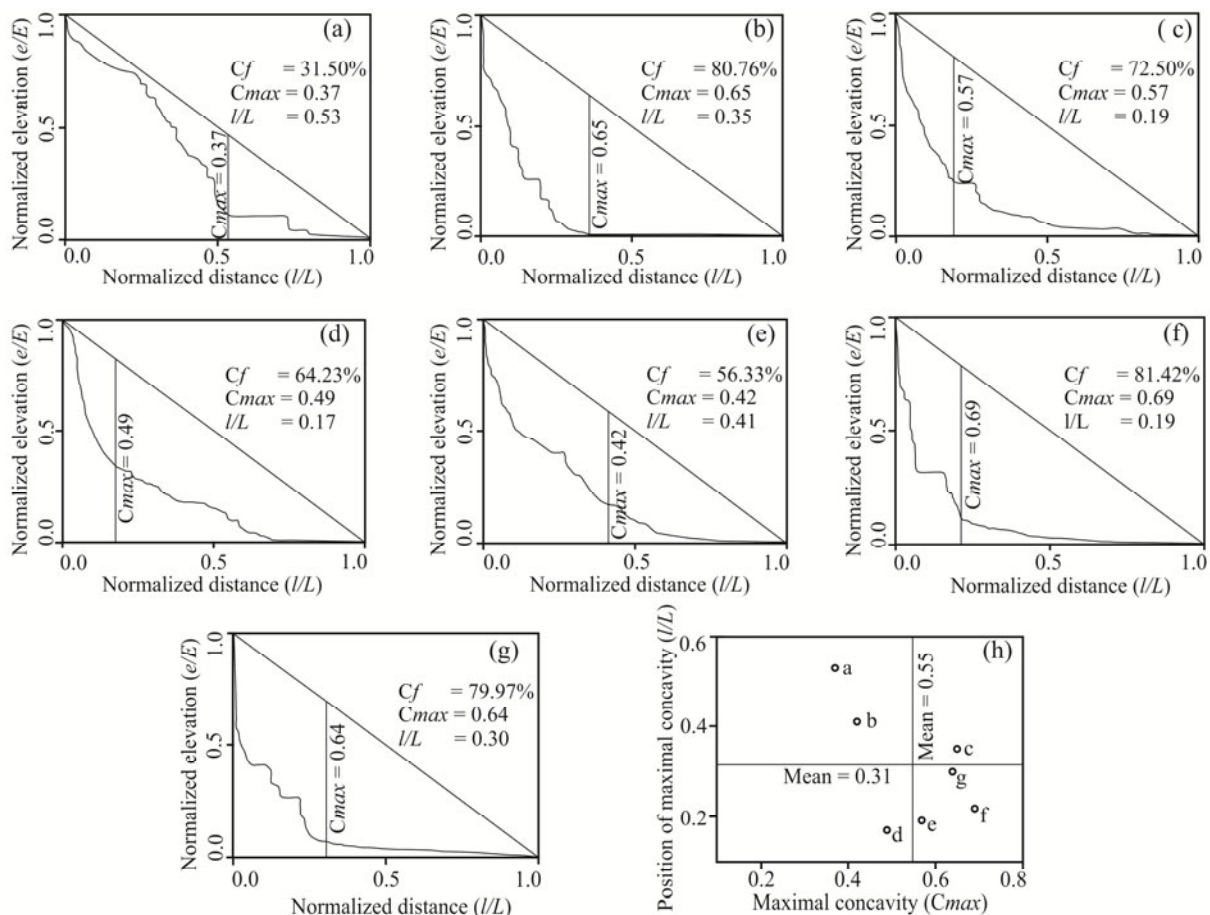


Figure 4 Normalized longitudinal profiles (refer to Figure 3 for location) for a) Subansiri River; b) Kamala River; c) major tributary of Kamala River; d) Ranga Nadi; e) Dikrong River; f) Jiadhah and g) Dimow River. C_f – longitudinal profile concavity factor, C_{max} - maximal concavity, l/L is the distance of the maximal concavity from the source of the river. In the Figure h the open circles with letter symbols represents the C_{max} - l/L plots following the serial number of the rivers given above.

in that area is presented in Table 1. The knickpoint distinctly positioned in the faults zones present in the Subansiri River basin.

3.4 Valley asymmetry factor (AF)

The Subansiri has the basin area to the right, $A_r = 16538 \text{ km}^2$ and total basin area $A_t = 35762 \text{ km}^2$, and the computed AF is 3.76. According to Pérez-Peña et al. (2010) classification the basin is symmetrical. But the shape of the basin (crescent shape) shows that the basin is structurally controlled. Hence valley asymmetry is computed for all the three parts of the basin and for all (30 numbers) 4th order basins. The AF computed for the upper and middle reaches are 2 ($A_t = 12394 \text{ km}^2$ and $A_r = 6426 \text{ km}^2$) and 25 ($A_t = 14460 \text{ km}^2$ and $A_r = 3672 \text{ km}^2$) respectively which establish that the middle part of the Subansiri basin is highly asymmetrical and it conforms the shift of the river towards northeast in this section. However, the upper part of the basin is symmetrical. The valley asymmetry factor of the 4th order sub-basins (Table 2; Figure 5b) shows that sub-basins falling in the northern periphery and southern periphery

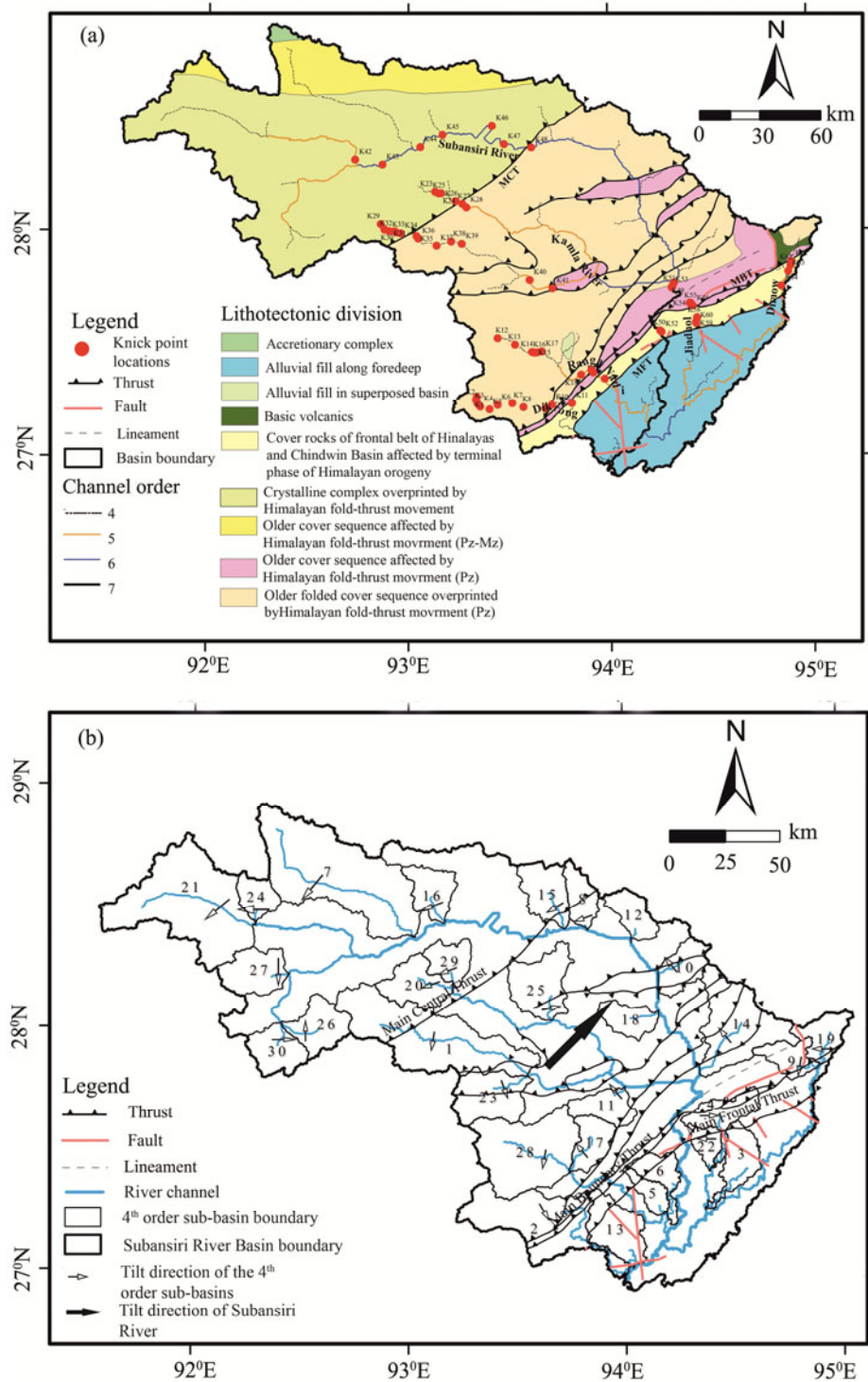


Figure 5 (a) Locations of the knickpoints on the Subansiri River and its tributaries Ranga Nadi, Kamala, Dikrong, Jiadhah, Dimow and tributary of Kamala. (b) The 4th order subbasins of Subansiri and tilting direction of the sub-basins as well the middle part of the Subansiri River Basin. MCT- Main Central Thrust, MBT- Main Boundary Thrust and MFT- Main Frontal Thrust. Numbers in figure (b) refer to the basins number of the 4th order Subansiri sub-basins. Abbreviations: Pz – Paleozoic; Mz – Mesozoic.

Table 1 Location of knickpoints along the longitudinal profiles of the Subansiri River and its tributaries the Kamala, the Ranganadi, the Dikrong, the Jiadhah, the Dimow and the tributaries of Kamala. MCT, MBT and MFT are the abbreviations of Main Central Thrust, Main Boundary Thrust and Main Frontal Thrust.

Sl. No	Knick points	Longitudinal profile	North lat. (°)	East long.(°)	Height diff.(m)	Associated structure	
1	K1	Dikrong	27.27	93.34	42	Between MBT and MCT	
2	K2		27.25	93.34	22		
3	K3		27.24	93.34	45		
4	K4		27.22	93.36	33		
5	K5		27.21	93.40	17		
6	K6		27.23	93.44	14		
7	K7		27.24	93.52	106		
8	K8		27.22	93.57	18		
9	K9		27.22	93.68	11		
10	K10		27.23	93.71	25		MBT zone
11	K11	27.24	93.81	36	Between MBT and MCT		
12	K12	27.53	93.44	20			
13	K13	27.50	93.53	83			
14	K14	27.47	93.61	19			
15	K15	27.46	93.63	19			
16	K16	27.47	93.64	43			
17	K17	27.47	93.66	48			
18	K18	27.36	93.86	95			
19	K19	27.39	93.91	67		MBT zone	
20	K20	27.38	93.91	84			
21	K21	27.37	93.92	26	North of MCT		
22	K22	27.35	93.98	26		MFT Zone	
23	K23	28.18	93.13	308			
24	K24	28.17	93.15	101			
25	K25	28.17	93.16	48			
26	K26	28.14	93.24	340			
27	K27	28.12	93.27	148		MCT Zone	
28	K28	28.11	93.29	79			
29	K29	28.04	92.86	568			
30	K30	28.01	92.88	30		North of MCT	
31	K31	28.00	92.90	62			
32	K32	28.00	92.93	66			
33	K33	28.00	92.94	106			
34	K34	27.99	92.96	60	MCT Zone		
35	K35	27.98	93.04	232			
36	K36	27.97	93.05	220			
37	K37	27.94	93.14	39			
38	K38	27.96	93.21	21			
39	K39	27.95	93.27	62			
40	K40	27.79	93.60	45			
41	K41	27.75	93.72	23			
42	K42	28.32	92.73	198			
43	K43	28.30	92.87	166			
44	K44	28.38	93.06	115	North of MCT		
45	K45	28.43	93.17	302			
46	K46	28.47	93.42	51			
47	K47	28.39	93.48	490			
48	K48	28.38	93.62	370		MCT Zone	
49	K49	27.77	94.32	315		MBT zone	
50	K50	Subansiri	27.56	94.25		101	Between MBT and MFT
51	K51		27.76	94.31		326	MBT zone
52	K52		27.55	94.26		95	Between MBT and MFT
53	K53		27.75	94.31		119	MBT zone
54	K54		27.69	94.40	10		
55	K55		27.68	94.41	59	MBT Zone	
56	K56		27.67	94.42	57		
57	K57		27.61	94.44	40		
58	K58		27.61	94.44	115		
59	K59		27.60	94.43	10		
60	K60	27.59	94.43	19			
61	K61	27.86	94.91	29	Between MBT and MFT		
62	K62	27.84	94.91	18			
63	K63	27.82	94.89	36			
64	K64	27.75	94.86	10			

Table 2 Basin parameters of 4th order sub-basins of Subansiri River. HI- Hypsometric Integral, V_f -Ratio of valley floor and height, AF -Asymmetry factor, A_r -the area of the basin to the right (facing downstream) of the trunk channel, and A_t -the total area of the drainage basin.

Basin No	HI	V_f	$AF1$	$AF2$
1	0.36	0.08	44.52	5.48
2	0.32	0.12	37.44	12.56
3	0.03	0.00	79.11	29.11
4	0.28	0.13	78.38	28.38
5	0.05	0.00	55.72	5.72
6	0.09	0.00	71.58	21.58
7	0.61	0.08	28.22	21.78
8	0.59	0.19	19.75	30.25
9	0.37	0.33	39.63	10.37
10	0.43	0.03	23.62	26.38
11	0.43	0.21	57.32	7.32
12	0.56	0.09	28.67	21.33
13	0.06	0.00	36.77	13.23
14	0.19	0.59	25.65	24.35
15	0.57	0.05	36.68	13.32
16	0.56	0.09	32.41	17.59
17	0.51	0.26	18.20	31.80
18	0.36	0.12	51.08	1.08
19	0.31	0.19	28.66	21.34
20	0.46	0.09	42.90	7.10
21	0.34	0.98	36.42	13.58
22	0.08	0.00	37.82	12.18
23	0.44	0.14	41.43	8.57
24	0.47	0.22	21.31	28.69
25	0.36	0.11	77.60	27.60
26	0.47	0.14	23.33	26.67
27	0.51	0.41	27.58	22.42
28	0.39	0.23	43.79	6.21
29	0.51	0.05	22.68	27.32
30	0.44	0.23	25.36	24.64

Notes: $AF1 = A_r/A_t \times 100$ (Keller and Pinter, 2002); $AF2 = |50 - A_r \times 100 / A_t|$ (Perez-Pena et al. 2010)

(north of the Jia-Bhareli Basin which is tectonically active) of the upper-Subansiri basin and the south-eastern and eastern parts of the basin show strongly asymmetrical basin ($AF > 15$). The values also indicate that the sub-basins falling in the MCT Zone possess higher AF values (Table 2 and Figure 5b) thereby giving strong asymmetry to the basins. The sub-basins of the western and south-western parts of the Subansiri possess lower AF (Table 2; Figure 5b) values indicating symmetrical to moderately asymmetrical basin shapes.

3.5 Valley profiles

Total of five valley profiles have been drawn from right bank to left bank where no contributory channel meets the main trunk in the Subansiri and the Kamala rivers (Figures 3 and 6). The valley

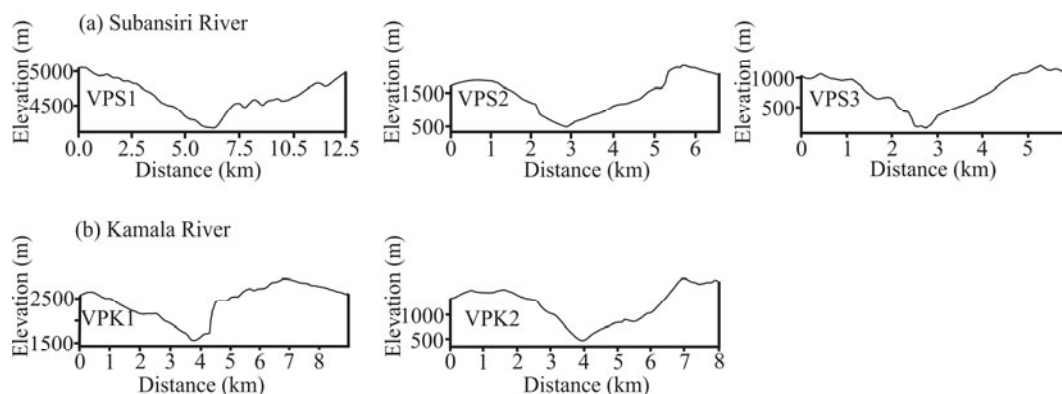


Figure 6 Valley profiles of the Subansiri River and its tributary the Kamala. Locations are indicated in Figure 3. VPS1, VPS2, VPS3 – Valley profiles of the Subansiri; VPK1, VPK2 – Valley profiles of the Kamala. Refer Figure 3 for the locations of the profiles.

profiles VPS3 and VPK2 show steep right bank and gentle left bank, while profiles VPS1, VPS2 and VPK1 show steep left banks.

3.6 Hypsometry

Out of the three 6th order sub-basins of the Subansiri, the northern sub-basin (sub-basin ii) has comparatively higher *HI* value (0.49) and convex upward hypsometric curve (Figure 7), whereas the other two sub-basins (i and iii) the *HI* values are markedly lower (0.26 and 0.11 respectively) with concave shaped hypsometric curves indicating erosion exceeding upliftment, or it can be inferred that these areas remain tectonically inactive for long period of time. The 4th (sub-basins 3, 5, 6, 13, 22, 28) (Figure 8) and 5th (sub-basins f, g) order sub-basins (Figure 7) of the Subansiri occupy alluvial plains of the Brahmaputra with low *HI* values (Figure 7) and concave down hypsometric curves. The *HI* of the 4th order sub-basins (7, 15, 16, 20, 26, 27, 29, 30) (Figure 8) indicate that the sub-basins of the upper Subansiri catchment possesses relatively high *HI* values and also S-shaped hypsometric curves indicating tectonically young topography in the sub-basins. The 4th order sub-basins *HI* values in the middle Subansiri basin are sufficiently high (sub-basin 8, *HI*=0.59; sub-basin 12, *HI* = 0.56) in

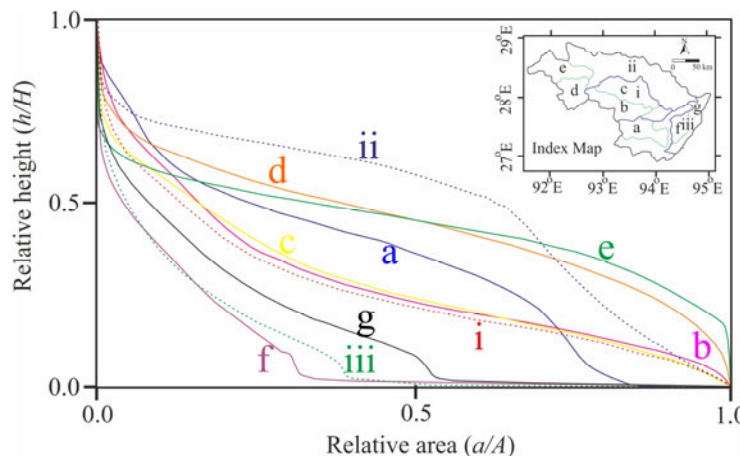


Figure 7 Percentage hypsometric curves of the 5th order (a to g, coded by same colour of the continuous curves with their respective sub-basin letterings) and 6th order (i to iii, coded by same colour of the dashed curves with their respective sub-basin letterings) of sub-basins of the Subansiri. The sub-basins are indicated in the inset index map. The hypsometric integral (*HI*) values for the sub-basins are, a = 0.34, b = 0.29, c = 0.29, d = 0.45, e = 0.44, f = 0.10, g = 0.16, i = 0.27, ii = 0.49, iii = 0.11. In the figure the relative area, *a/A* is the ratio of the area between a contour and the upper perimeter (area 'a') to the total drainage basin area (area *A*); and the relative height, *h/H* is the ratio of the height of the contour above base (*h*) to the total height of basin (*H*). In the index map the blue lines are the boundaries of the 6th order sub-basins and the green lines are the boundaries of the 5th order sub-basins.

the eastern part indicating tectonically young topography, whereas the western sub-basins 11 (*HI* = 0.43) and 23 (*HI* = 0.44) have comparatively eroded landform. The central part of the reach containing the sub-basins 18 (*HI* = 0.36) and 25 (*HI* = 0.36) indicate pronounced erosion along the river course. The sub-basin 8 is within the MCT zone (Figure 8) where the river takes an easterly course (Figure 8) and then it takes a sharp turn to

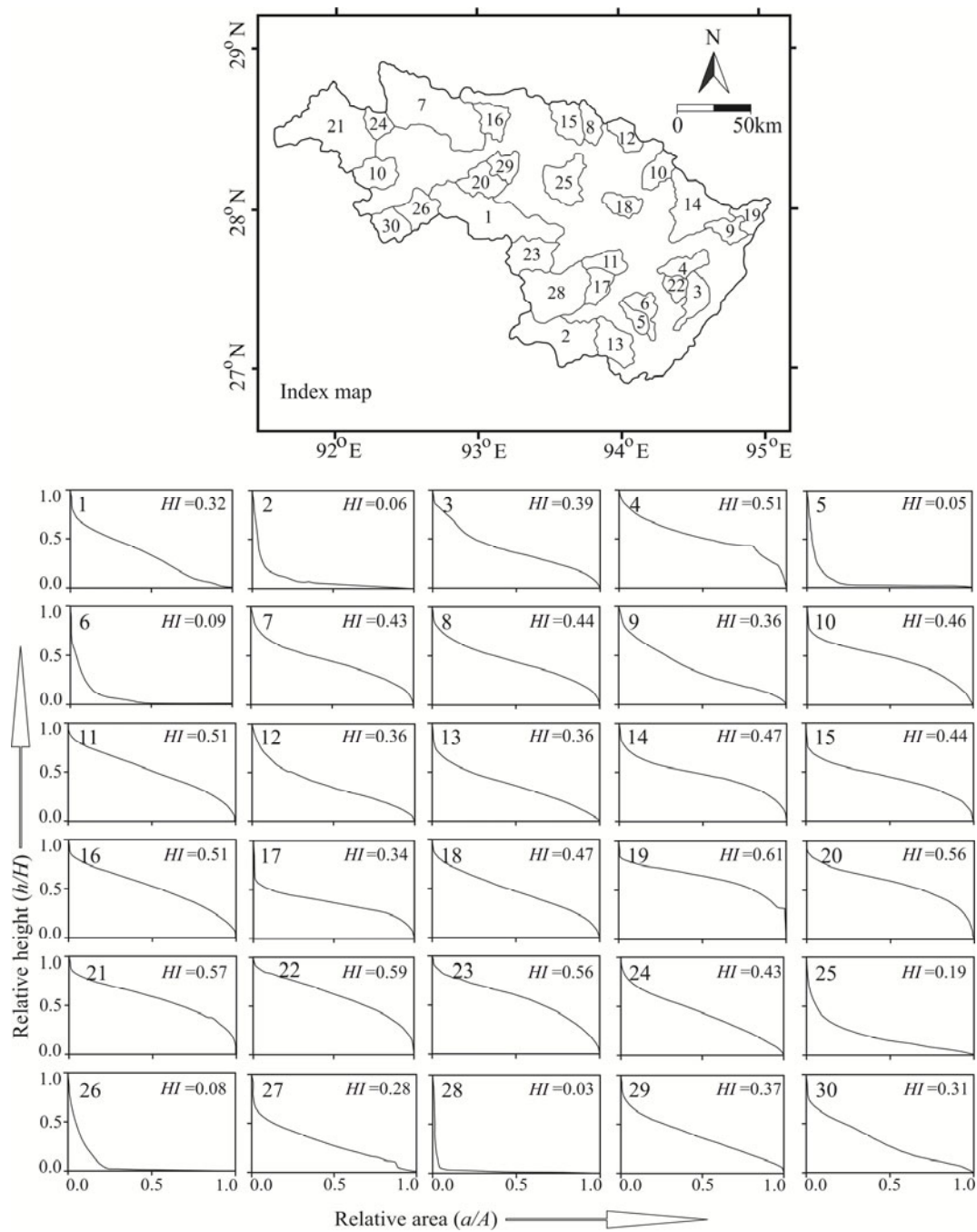


Figure 8 Percentage hypsometric curves of 4th order in sub-basins (1 to 30) of the Subansiri. Location of the sub-basins is indicated in the index map on the top of the figure. *HI* is the hypsometric integral index. In the figure the relative area, a/A is the ratio of the area between a contour and the upper perimeter (area ‘ a ’) to the total drainage basin area (area A); and the relative height, h/H is the ratio of the height the contour above base (h) to the total height of basin (H).

flow to the south near Chepcha, the area being represented by the sub-basin 12.

3.7 Transverse topographic symmetry (T)

The transverse topographic symmetry (T) is

determined in the lower alluvial reach of the Subansiri. T is calculated along two sections (T_1 and T_2 , Figure 3) with values $T_1 = 0.47$ ($D_a = 29$ km and $D_d = 61$ km) and $T_2 = 0.59$ ($D_a = 25$ km and $D_d = 61$ km) indicating pronounced transverse asymmetry in the lower reach of the river.

3.8 Valley floor width-height ratio (V_f)

The V_f values vary from 0.03 (sub-basin 10) to 0.98 (sub-basin 21) (Table 2). The V_f values are significantly large for the sub-basins covering glaciated landform (sub-basins 21 and 27, Table 2) with wide U-shaped valley, and the sub-basins (9 and 14) placed in between MBT and MFT, the zone comprises of the rocky terrains of southern part of the older folded cover sequences overprinted by Himalayan fold thrust movement, older cover sequences affected by Himalayan fold thrust movement of Paleozoic age and cover rocks of frontal belt of Himalaya affected by fold thrust movement during terminal phase of Himalayan orogeny. Intermediate values are found in the central part of the middle Subansiri (4th order sub-basins 2, 11, 17, 18, 23, 24 and 25) and southern part of the upper Subansiri basin (4th order sub-basins 26 and 30, and conspicuous lower V_f values are found for the 4th order sub-basins 8, 10, 12, 15, 16 and 29 (Figure 8 for location).

3.9 Stream length gradient (SL)

SL indices have been calculated for the 4th, 5th, 6th and 7th order streams of the Subansiri River and a comparative study of these values with the lithotectonics of the region have been made. The SL indices have higher values in upper part (>3500-167000 gradient meter; Figure 9a) and lower values in the middle part of the Subansiri basin (0-3500 gradient meter; Figure 9a). The SL index is higher in those areas where the channels cross MCT (>6500 gradient meter) and MBT (>6500 gradient meter). In the study it is also observed that the local slope, $\Delta H/\Delta L$ of the Subansiri ranges between 1/1000 to 1/100 in general, but anomalous values can be seen in few localities in the upper part (1/75 to <1/10), across MCT (1/50 to 1/10) and across MBT (1/75 to 1/25) in several places. The stream length profiles for the Subansiri (Figure 9b) and its largest tributary Kamala (Figure 9c) have been drawn where distance from the basin divides in 'log_e' scale were plotted against altitude (meter) in arithmetic scale. In those plots average SL indices have also been calculated for few segments. The average SL index has higher value in the segment from the north of the MCT to the mid-section of the middle Subansiri basin. There are few classification systems (El Hamdouni et al.

2008; El Hamdouni et al. 2010; Dubey and Shankar 2019) that have been proposed but as in this study the river channels are much longer so the SL index values changes drastically with the changing L values. Moreover El Hamdouni et al. (2008) classified the SL index value in combination with rock strength, but in our case the index changes within the same rock types and geology of the Higher Himalayan part of Arunachal Himalaya. In the present study the SL index classes are pinned at 3500 gradient meter where abrupt gradient changes are noticed across the MCT in the western part of the basin.

4 Discussion

The morphometric analysis of the Subansiri basin shows that the basin possesses areas with different morphometric behaviours. It is evident from the results that the northern, eastern, central parts of the upper and middle Subansiri basins possess young, rugged topography with deeply incised valleys, asymmetrical basins, uplifted terrains, and convex longitudinal profiles. Further south in the western part of the lower middle Subansiri basin and foothill region show smooth and matured topography. The relief and slope variant maps show that the MCT zone, upper middle Subansiri basin north of MCT and the eastern periphery of the basin has higher values indicating rugged topography with high relief. The rectangular drainage patterns in the upper and middle reaches of the Subansiri basin (Figure 3) are caused by the presence of joints, faults and thrusts. The S-shaped hypsometric plots and high HI values distribution pattern of the 4th, 5th and 6th order sub-basins give an expression that in the northern, western and eastern periphery areas both within and outside the basin boundary have been uplifted relatively at higher rate. The low value of V_f and high SL index of the sub-basins suggest high uplift as well as high incision rate in the upper catchment of the Subansiri in its northern and eastern areas. Few sub-basins on the glacial landforms in the upper Subansiri catchment have lower V_f and SL indices. The general trend of the valley profiles with steeper right bank and gentle left bank indicating that the upper part of Subansiri basin has northerly tilt and the middle part has

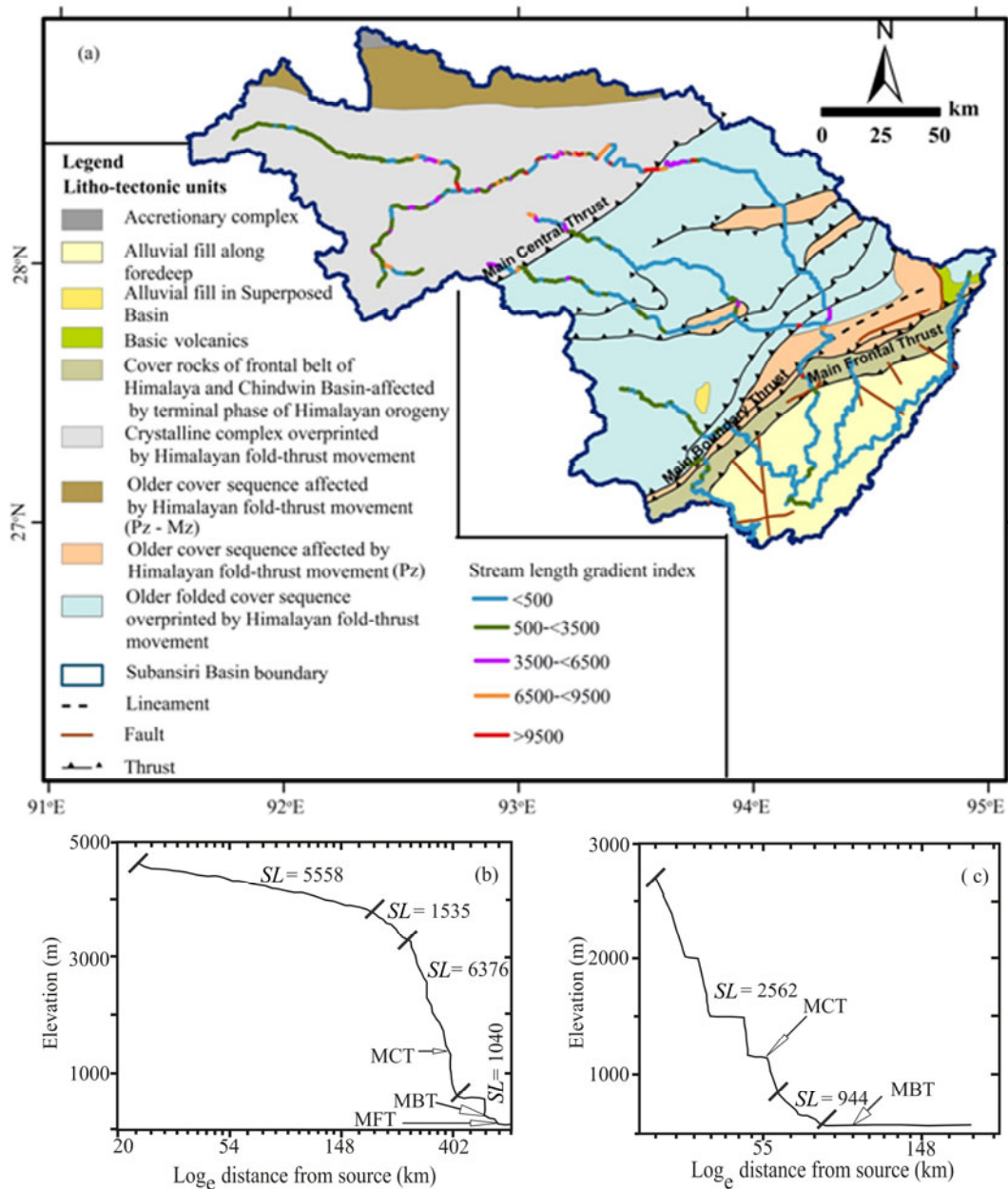


Figure 9 (a) Stream length gradient index map of (4th, 5th, 6th and 7th order rivers) of Subansiri River and its major tributaries. Profiles of Subansiri (b) and Kamala (c) rivers. The average SL (*Stream length gradient index*) values are indicated in the profile plots in the sections indicated by the dashed lines. MCT, MBT and MFT (marked by continuous lines across the stream profiles) are the positions of Main Central Thrust, Main Boundary Thrust and Main Frontal Thrust in the profiles. *Abbreviations*: Pz – Paleozoic; Mz – Mesozoic.

easterly tilt. The normalized longitudinal profiles and concavity parameters of the Subansiri and its tributaries show that except the Subansiri River's main trunk channel all the tributaries are graded streams with maximum concavity (0.42-0.69) positioned from the upper to middle part (0.19-0.41) of the reach, while the Subansiri River's main trunk is least graded with convex longitudinal profiles and attains its maximum convexity in the

middle reach ($C_{max} = 0.37$ at $\Delta d/D = 0.53$). The knickpoints in the longitudinal profile of the Subansiri give precise locations of the tectonic thrust zones, *viz.*, MFT, MBT and MCT within the river basin.

The valley asymmetry factor of the Subansiri, calculated for the whole basin considering as a single entity is almost negligible (4%), and when it is considered into the sub-reaches, it unmistakably

consists of symmetrical upper reach, and remarkable asymmetry ($AF = 25\%$) in the middle reach, and the river is shifted towards east. This middle reach of the river is located in the lithotectonic zone bounded by MCT to the north and MBT to the south. The valley asymmetry of the 30 numbers of 4th order sub-basins appears to be caused by these two major tectonic elements. The derived transverse topographic symmetry index (T) shows that the lower Subansiri basin has eastward tilting.

The locations of earthquake epicentres in the river basin and its immediate surroundings (Figure 1) indicate three active tectonic domains marked as A, B and C in Figure 1. Earthquakes are caused by rigid deformation of the crust through release of strain and have considerable influence in evolving shape of a basin as happened in the Subansiri basin. The north-western part of the basin along with the eastern part of the Jia-Bhareli Basin marked as A (Figure 1) has records of frequent earthquakes during the instrumentally recorded earthquake period. The tectonic domain that extends from further south of the MCT to the alluvial plains of the Brahmaputra with remarkably less number of earthquakes is marked as tectonic domain B (Figure 1) and is the seat of the lower reach of the Subansiri. The tectonic domain covering the east, central part of the basin extending the eastern catchment boundary along with the Siang window where Main Himalayan belt abuts against the Mishimi Massif formed the tectonic domain marked as C in Figure 1. The lower part of the basin is tectonically inactive and dormant which yielded a few micro-earthquakes south of the MFT as recorded and has been identified as the Eastern Himalaya's seismic gap (Khattri 1987). As earthquakes are the reflection of accumulation and release of tectonic stress due to on-going tectonic movement in an area, these results are reassuring the findings of morphometric analyses in the basin. The lower Subansiri basin (tectonic domain B, Figure 1) with matured topography mainly composed of older cover sequences affected by Himalayan fold-thrust movements, older folded cover sequences overprinted by Himalayan fold-thrust movement and cover rock of frontal belt of Himalaya affected by fold-thrust movement during terminal phase of the Himalayan Orogeny. These

lithotectonic assemblages are mainly represented by low grade metamorphic and sedimentary rocks. In Arunachal Pradesh, the foothill region witnesses maximum precipitation (Dhar and Nandargi 2004), and so here erosional processes predominate over the tectonic processes. The rare occurrence of earthquake in this area illustrates that the area is tectonically not active.

5 Conclusion

The study establishes that the Subansiri River Basin evolved through time and space due to pronounced tectonic activities in the eastern Himalayas. The predominant tectonic movements in the western part of the basin have resulted in tilting of the basin towards north in the upstream, and towards east in the middle and lower parts. The upper and middle parts of the basin have rugged and uplifted topography, highly incised, tilted basinal area caused by active tectonism. The study also establishes that the morphometric and hypsometric data generated from SRTM DEM combined with seismic and tectonic data form important tools to understand tectonic landform evolutionary processes in a tectonically active region.

Acknowledgements

The authors are thankful to the Department of Geological Sciences, Gauhati University, Assam, India for providing the necessary laboratory supports to carry out the study. We offer our gratitude to DST, Govt. of India for the FIST (2016-2021) project funding to the Department of Geological Sciences to develop the laboratories. We acknowledge the services provided by the USGS website for source of the SRTM DEM data and the earthquake catalogue. We are also thankful to the ISC portal and NEIST, Jorhat, Assam, India for providing earthquake catalogue. The authors are very much thankful to the anonymous reviewers for their suggestions to improve the research article.

References

- Adediran AO, Parcharidis I, Poscolieri M, et al. (2004) Computer-assisted discrimination of morphological units on north-central Crete (Greece) by applying multivariate statistics to local relief gradients. *Geomorphology* 58: 357-370.
- Alipoor R, Poorkermani M, Zare M, et al. (2011) Active tectonic assessment around Rudbar Lorestan dam site, High Zagros Belt (SW of Iran). *Geomorphology* 128: 1-14.
- Angelier J, Baruah S (2009) Seismotectonics in Northeast India: a stress analysis of focal mechanism solution of earthquakes and its kinematic implications. *Geophysical Journal International*. <https://doi.org/10.1111/j.1365-246X.2009.04107.x>
- Azor A, Keller EA, Yeats RS (2002) Geomorphic indicators of active fold growth: South Mountain–Oak Ridge Ventura basin, southern California. *Geological Society of America Bulletin* 114: 745-753.
- Ben-Menahem A, Aboodi E, Schild R (1974) The source of the great Assam earthquake - an interplate wedge motion. *Physics of the Earth and Planetary Interiors* 9: 265-289.
- Bilham R, England P (2001) Plateau 'pop up' in the great 1897 Assam earthquake. *Nature* 410: 806-809.
- Bloom AL (2003) *Geomorphology: A Systematic Analysis of Late Cenozoic Landforms*. Pearson Education, pp. 268-272.
- Brocklehurst S, Whipple K (2002) Glacial erosion and relief production in the Eastern Sierra Nevada, California. *Geomorphology* 42:1-24
- Bull WB, McFadden LD (1977) Tectonic geomorphology north and south of the Garlock fault, California. In: Doehring, DO, (eds.) *Geomorphology in Arid Regions*, Proceedings of the Eighth Annual Geomorphology Symposium. State University of New York, Binghamton, pp. 115-138.
- Bull WB (1978) Geomorphic Tectonic Classes of the South Front of the San Gabriel Mountains, California. U.S. Geological Survey Contract Report, 14-08-001-G-394, Office of Earthquakes, Volcanoes and Engineering, Menlo Park, CA.
- Burbank DW, Anderson RS (2001) *Tectonic Geomorphology*. Wiley Blackwell Press, 411p.
- Cox RT (1994) Analysis of drainage basin symmetry as a rapid technique to identify areas of possible quaternary tilt-block tectonics: an example from the Mississippi Embayment. *Geological Society of America Bulletin* 106: 571-581.
- Das JD (2004) Active tectonics of the Eastern Himalayas foothills region and adjoining Brahmaputra Basin based on satellite images. *International Journal of Remote Sensing* 25 (3): 549-557.
- Dehbozorgi M, Pourkermani M, Arian M, et al. (2010) Quantitative analysis of relative tectonic activity in the Sarvestan area, central Zagros, Iran. *Geomorphology* 121: 329-341.
- Della Seta M, Del Monte M, Fredi P, et al. (2008) Morphotectonic evolution of the Adriatic piedmont of the Apennines: advancement in the knowledge of the Marche–Abruzzo border area. *Geomorphology* 102: 119-129.
- Demoulin, A. (1998) Testing the tectonic significance of some parameters of longitudinal river profiles: the case of the Ardenne (Belgium, NW Europe). *Geomorphology* 24(2-3): 189-208.
- Dhar ON, Nandargi S (2004) Rainfall distribution over the Arunachal Pradesh Himalayas. *Weather* 59(6): 155-157.
- Duarah BP, Phukan S (2011) Seismic hazard assessment in the Jia Bhareli river catchment in eastern Himalaya from SRTM-derived basin parameters, India. *Natural Hazards*. <https://doi.org/10.1007/s11069-011-9761-4>
- Dubey RK, Shankar R (2019) Drainage Pattern and its Bearing on Relative Active Tectonics of a Region: A Study in the Son Valley, Central India. *Journal of the Geological Society of India* 93(6): 693-703.
- GSI (2000) *Seismotectonics Atlas of India and its Environs*. In: Narula PL, Acharyya SK, Banerjee J (eds.) *Geological Survey of India, Special publication Series* - 59.
- Hack JT (1973) Stream-profile analysis and stream-gradient index. *Journal of Research of the U.S. Geological Survey* 1(4): 421-429.
- Hamdouni E, Irigaray R, Fernández C, et al. (2008) Assessment of relative active tectonics, southwest border of the Sierra Nevada (southern Spain). *Geomorphology* 96: 150-173.
- Hamdouni E, Irigaray R, Jiménez-Perálvarez JD, et al. (2010) Correlations analysis between landslides and stream length gradient (SL) index in the southern slopes of Sierra Nevada (Granada, Spain). In: Williams et al., eds. *Geologically Active*, Taylor & Francis Group, London, ISBN 978-0-415-60034-7.
- Hancock GR, Martinez C, Evans KG, et al. (2006) A comparison of SRTM and high-resolution digital elevation models and their use in catchment geomorphology and hydrology: Australian examples. *Earth Surf Process Landforms* 31: 1394-1412.
- Howard AD (1967) Drainage analysis in geological interpretation: A summation. *American Association Petroleum Geologists Bulletin* 51: 2246-2259.
- ISC (2007) *Bulletin of the International Seismological Centre, event catalogue search*. <http://www.isc.ac.uk/iscbulletin/search/catalogue/> (Accessed on 17 April, 2018).
- Kaushal RK, Singh V, Mukul M, et al. (2017) Identification of deformation variability and active structures using geomorphic markers in the Nahan salient, NW Himalaya, India. *Quaternary International* 462: 194-210.
- Kayal JR (1998) Seismicity of Northeast India and surroundings - development over the past 100 years. *Journal of Geophysics* 19 (1): 9-34.
- Keller EA, Pinter N (2002) *Active tectonics: earthquake, uplift, and landscape* (2nd ed). Prentice Hall, Englewood Cliffs. 362p.
- Khattri KN (1987) Great earthquakes, seismicity gaps and potential for earthquake disaster along the Himalaya plate boundary. *Tectonophysics* 138(1): 79-92.
- Kumar D, Duarah BP (2019) Neo-tectonic signatures in the Mishmi Massif, Eastern Himalayas: an interpretation on the basis of the Lohit River Basin geometry. *Arabian Journal of Geosciences* 12. <https://doi.org/10.1007/s12517-019-4851-9>
- Leeder MR, Jackson JA (1993) The interaction between normal faulting and drainage in active extensional basins with example from Western United States and Central Greece. *Basin Research* 5: 79-102.
- Liu Y (2008) An evaluation on the data quality of SRTM DEM at the Alpine and plateau area, North-western of China. *The International Archives of the Photogrammetry, Remote Sensing and Spatial Information Sciences*. Beijing XXXVII (Part B1): 1123-1127.
- Long S, McQuarrie N, Tobgay T, et al. (2011) Tectono-stratigraphy of the Lesser Himalaya of Bhutan: Implications for the along strike stratigraphic continuity of the northern Indian margin. *Geological Society of America Bulletin* 123 (7/8): 1406-1426. <https://doi.org/10.1130/B30202.1>
- Mahmood SA, Gloaguen R (2012) Appraisal of active tectonics in Hindu Kush: Insights from DEM derived geomorphic indices and drainage analysis. *Geoscience Frontiers* 3(4): 407-428.
- Maroukian H, Gaki-Papana K, Karymbalis E, et al. (2008) Morphotectonic control on drainage network evolution in the Perachora Peninsula, Greece. *Geomorphology* 102: 81-92.
- Matoš B, Perez-Peña, José V, et al. (2016) Landscape response to recent tectonic deformation in the SW Pannonian Basin: Evidences from DEM-based morphometric analysis of the Bilogora Mt. area, NE Croatia. *Geomorphology*. <https://doi.org/10.1016/j.geomorph.2016.03.020>
- Misra DK (2012) Active faults in the eastern syntaxial bend, Arunachal Pradesh, India. *Himalayan Geology* 33(2): 146-150.
- Molin P, Pazzaglia FJ, Dramis F (2004) Geomorphic expression of active tectonics in a rapidly-deforming fore-arc, Sila massif, Calabria, southern Italy. *American Journal of Science* 304: 559-589.
- Mukul M, Srivastava V, Mukul M (2016) Out-of-sequence

- reactivation of the Munsiri thrust in the Relli River basin, Darjiling Himalaya, India: Insights from Shuttle Radar Topography Mission digital elevation model-based geomorphic indices. *Geomorphology*.
<https://doi.org/10.1016/j.geomorph.2016.10.029>
- NEIST (2012) Earthquake Catalogue in and around North Eastern Region of India (including Historical earthquakes). First Interim Report (Medieval Period to 1999 (part 1) and 2000-2013 (part 2)); RGR/ASDMA/53/2010/pt./206; North East Institute of Science and Technology. pp 1-225.
- Oldham RD (1899) Report on the Great Earthquake of 12 June 1897, Memoir, Geological Society of India. 29: pp. 379.
- Ollier CD (1981) Tectonics and landforms. Longman Group limited, Harlow, England. p 324.
- Pérez-Peña JV, Azor A, Azañón JM, Keller EA (2010) Active tectonics in the Sierra Nevada (Betic Cordillera, SE Spain): Insights from geomorphic indexes and drainage pattern analysis. *Geomorphology* 119: 74-87.
- Poddar MC (1950) Preliminary report of the Assam earthquake of 15th August 1950. *Geological Survey of India Bulletin Series B 2*: 1-40.
- Rivix (2005) Rivers tools (Topographic and river network analysis) version 3.0 user's guide. www.rivix.com and www.rivertools.com (Accessed on 25 July 2012).
- Rajendran CP, Rajendran K, Duarah BP, et al. (2004): Interpreting the style of faulting and paleoseismicity associated with the 1897 Shillong, northeast India earthquake: implications for regional tectonism. *Tectonics* 3(4).
<https://doi.org/10.1029/2003TC001605>
- Rockwell TK, Keller EA, Johnson DL (1985) Tectonic geomorphology of alluvial fans and mountain fronts near Ventura, California. In: Morisawa M (eds.), *Tectonic Geomorphology*. Proceedings of the 15th Annual Geomorphology Symposium. Allen and Unwin Publishers, Boston MA. pp183-207.
- Rădoane M, Rădoane N, Dumitriu D (2003) Geomorphological evolution of longitudinal river profiles in the Carpathians. *Geomorphology* 50: 293-306.
- Ruszkiczay-Rüdiger Z, Fodor L, Horváth E, et al. (2009) Discrimination of fluvial, eolian and neotectonic features in a low hilly landscape: A DEM-based morphotectonic analysis in the Central Pannonian Basin, Hungary. *Geomorphology* 104: 203-217.
- Schumm SA, Dumont JF, Holbrook JMJ (2000) *Active tectonic and alluvial river*. Cambridge University Press, London. pp 4-11.
- Silva PG, Goy JL, Zazo C, et al. (2003) Fault generated mountain fronts in Southeast Spain: geomorphologic assessment of tectonic and earthquake activity. *Geomorphology* 250: 203-226.
- Srivastava V, Mukul M, Mukul M (2017) Quaternary deformation in the Gorubathan recess: Insights on the structural and landscape evolution in the frontal Darjiling Himalaya. *Quaternary International* 462: 138-161.
- SRTMFill (2003) SRTMFill is a fast and easy program for patching NULL-data holes in SRTM DEMs by progressively in-filling from surrounding data, quickly making usable data from unusable DEMs.
<http://3dnature.com/index.php/downloads/srtmfill-tool/> (Accessed on 12 May 2012).
- Strahler AN (1952) Hypsometric (Area-Altitude) analysis of Erosional topography. *Geological Society of America Bulletin* 63: 1117-1142.
- Tandon AN (1955) Direction of Faulting in the great Assam earthquake of 15 August 1950. *Indian Journal Meteorology and Geophysics* 6: 61-64.
- Twidale CR (2004) River patterns and their meaning. *Earth-Science Reviews* 67(3-4): 159-218.
- Thornbury WD (1989) *Principles of geomorphology*, 2nd edition. New Delhi: Wiley Eastern Ltd., pp. 119-125.
- Troiani F, Della Seta M (2008) The use of the stream length-gradient index in morphotectonic analysis of small catchments: a case study from Central Italy. *Geomorphology* 102: 159-168.
- USGS (2017) Unites State Geological Society Earthquake hazard programme. <https://earthquake.usgs.gov/earthquakes/search/> (Accessed on 7 December 2017).
- Yin A (2006) Cenozoic tectonic evolution of the Himalayan orogen as constrained by along-strike variation of structural geometry, exhumation history, and foreland sedimentation. *Earth Science Review* 76:1-131.
<https://doi.org/10.1016/j.earscirev.2005.05.004>